Interatomic resonant Auger effect in N_2O

Sascha Deinert,[1] Alexander Schrodt,[2] Gregor Hartmann,[1,2,3] Alexander Achner,[4,5] Anton N. Artemyev,[2] Arno Ehresmann,[2] Andreas Hans,[2] Markus Ilchen,[2,4] Leif Glaser,[1] Frank Scholz,[1] Jörn Seltmann,[1] Jens Viefhaus,[1,3] Philipp V. Demekhin,[2,*] and André Knie[2,†]

[1] *Deutsches Elektronen-Synchrotron DESY, Notkestraße 85, 22607 Hamburg, Germany*
[2] *Institut für Physik und CINSaT, Universität Kassel, Heinrich-Plett-Straße 40, 34132 Kassel, Germany*
[3] *Helmholtz-Zentrum Berlin für Materialien und Energie HZB, Hahn-Meitner-Platz 1, 14109 Berlin, Germany*
[4] *European XFEL GmbH, Holzkoppel 4, 22869 Schenefeld, Germany*
[5] *The Hamburg Centre for Ultrafast Imaging, Luruper Chaussee 149, 22761 Hamburg, Germany*

(Dated: August 5, 2020)

The interatomic resonant Auger effect in N_2O is investigated experimentally and theoretically. We observe variations of the ratio between the yields of 1s-photoionization of the central and terminal nitrogen atom in the photon energy range across the O $1s \rightarrow \pi^*$ excitation. The present *ab initio* calculations of electronic structure and dynamics attribute these variations to the Fano interference between the direct N 1s-photoionizations and the resonant O $1s \rightarrow \pi^*$ excitation followed by Auger decays into the respective core-shell continua. The theory reveals that this interatomic core-hole-transfer effect is governed entirely by an energy transfer mechanism, and not by charge transfer.

I. INTRODUCTION

Almost twenty years ago, a series of independent studies [1–3] demonstrated that core-level photoemission in solids is enhanced when scanning the ionization energy across the resonant core-level absorption range of a different neighboring atom. This phenomenon was termed multiatom resonant photoemission (MARPE), and its application for the determination of the local environment of an atom in a solid was demonstrated [4, 5]. For isolated molecules in the gas phase, MARPE can be understood as a nonlocal resonant Auger effect, where the core-excitation of one of the atoms is embedded in the core-level ionization continuum of another atom. In molecules, this effect was first identified in the differential photoionization cross section via nondipole photoemission from core-levels of N_2O and OCS molecules [6, 7]. To distinguish the short-range molecular process from the somewhat longer-range MARPE process, this phenomenon was termed nearest-neighbor-atom core-hole transfer (NACHT) effect.

Later on, this effect was successfully identified by other authors in NO and CS_2 molecules [8, 9]. They suggested to interpret it as a Fano interference between the direct and resonant ionization pathways in the nonlocal resonant Auger decay channel. In the coincident experiments of Refs. [8, 9], the Fano interference resulted in a clear enhancement of the on-resonance photoemission from those linear molecules (as compared to the off-resonance case) if they were oriented perpendicular to the light polarization direction, as they were addressing π^* resonances. On the contrary, no enhancement in photoemission was observed if the molecules were oriented in parallel with the light polarization. The authors proposed an analogy to the interatomic Coulombic decay (ICD, [10]). They also understood that the core hole is not transferred between two neighbours, but rather an energy transfer takes place. Therefore, they avoided the abbreviation NACHT and termed this phenomenon interatomic resonant Auger effect.

In the present work, we investigate the Fano interference between the direct and resonant photoionization pathways in the interatomic resonant Auger decay of N_2O. The processes relevant for the present study are schematically illustrated in Fig. 1 (see caption for details). In particular, as illustrated in this figure, we investigate the Fano interference between the pathways (a)+(b or c) and (d) for the central nitrogen atom, and between the pathways (a)+(e) and (f) for the terminal nitrogen. Our study allows to quantitatively compare the different interpretations of this effect in the originally investigated N_2O molecule by revealing the energy-transfer mechanism in the photoionization cross-section rather than in the nondipole parameter. By using state-of-the-art experimental and theoretical methods we demonstrate, that this effect causes variations in the ratio between the total 1s-photoionization yields of the central and terminal nitrogen atoms across the O $1s \rightarrow \pi^*$ resonance. We also suggest a straightforward analogy of this effect to the antenna-receiver mechanism [11] observed in the resonant ICD of heteronuclear dimers [12, 13].

II. EXPERIMENT

The experiment was performed at the P04 beamline [14] in the timing mode of the synchrotron radiation facility PETRA III at DESY in Hamburg, Germany. The APPLE II undulator was set to pure circular polarization to rule out angle dependent effects. The exit slit of the monochromator was set to 60μm. The photon en-

*Electronic address: demekhin@physik.uni-kassel.de
†Electronic address: knie@physik.uni-kassel.de

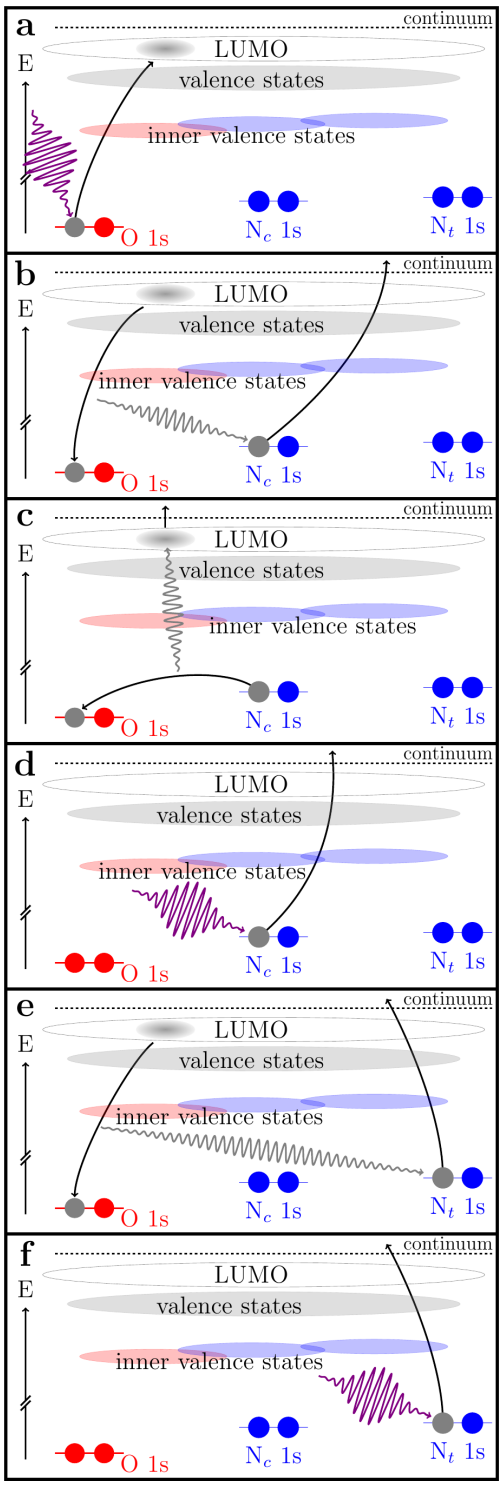

FIG. 1: Sketch of the presently studied processes: (a) excitation of an O 1s-electron into the π^* resonance; (b) interatomic participator Auger decay into the N_c 1s-continuum via the dominant energy transfer and (c) via the very weak charge transfer mechanisms; (d) direct ionization of the N_c 1s-electron; (e) interatomic participator Auger decay into the N_t 1s-continuum via energy transfer (charge transfer is here negligible); (f) direct ionization of the N_t 1s-electron. The Fano interference emerges for the N_c atom between the (a)+(b or c) and (d) pathways, and for N_t between (a)+(e) and (f).

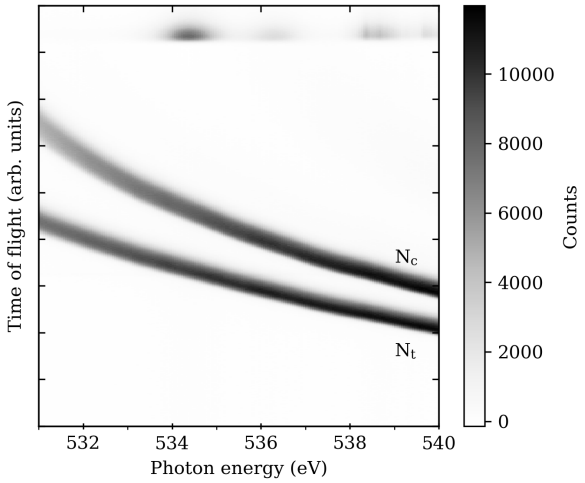

FIG. 2: False gray-scale plot of the excitation energy dependent photoelectron time-of-flight spectra in the region of the nitrogen 1s-photoelectron lines. The two prominent features are the terminal (lower inclining spectrum) and central (upper inclining spectrum) nitrogen 1s-photoelectron lines. The very fast conventional resonant Auger electrons released by the subsequent excitation pulse, seen at longer times of flight (on the top), were used for the exciting-photon energy calibration.

ergy was varied from 531 to 540 eV in steps of 50 meV across the O $1s \rightarrow \pi^*$ resonance, which is located at 534.6 eV [6]. For each individual step, a time-of-flight electron spectrum was recorded using a magnetic-bottle spectrometer described in detail in Ref. [15]. We focused on the ratio between the 1s-ionization yields of the central and terminal nitrogen atoms. Since it allows to neglect fluctuations of photon flux, target density, etc., i.e., is intrinsically calibrated. For the present exciting-photon energy range, the nominal kinetic energies of the N_c and N_t 1s-photoelectrons are in between 118 and 132 eV. The overall transmission of the spectrometer with these settings is much lower for electrons of kinetic energies as high as few hundreds of electron volts, as compared to low kinetic energies of few electron volts. In order to efficiently record the N_c and N_t 1s-photoelectrons and to resolve the 4 eV chemical shift between these photoelectron lines, a 114.5 V retardation field was applied.

Figure 2 shows a plot of the recorded time-of-flight spectra in the vicinity of the oxygen $1s \rightarrow \pi^*$ resonance. The two prominent lines can be identified as the N_c and N_t 1s-photoelectrons, respectively, at longer and shorter times of flight (note that the latter electrons have about 4 eV higher kinetic energies than the former). Very fast conventional resonant Auger electrons released by the subsequent excitation pulse were also detected, but with much lower probability due to the reduced transmission (nominal kinetic energies on the resonance are about 450–520 eV). Those electrons are seen on the top of Fig. 2 at larger times of flight. As one can see, this spectrum of

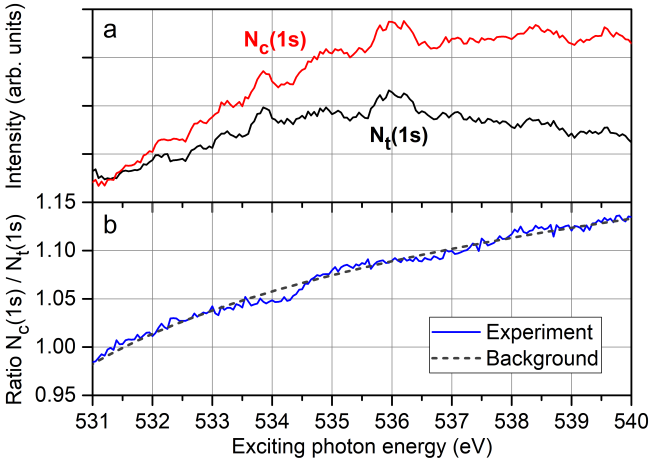

FIG. 3: Experimental results: (a) relative 1s-photoionization spectra for the central and terminal nitrogen atoms; (b) ratio of the $N_c(1s)$ to $N_t(1s)$ intensities and best fit of the logarithmic background.

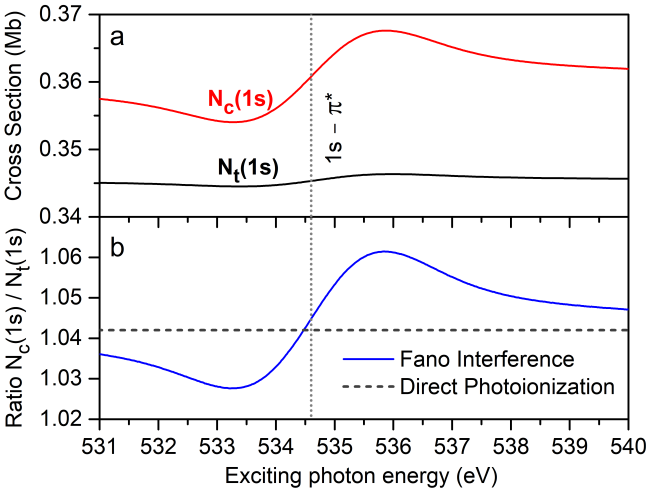

FIG. 4: Theoretical results: (a) cross sections for the 1s-photoionization of the central and terminal nitrogen atoms; (b) ratio between the $N_c(1s)$ and $N_t(1s)$ cross sections (solid curve). Only the O $1s \rightarrow \pi^*$ resonance was included in the calculations. Its position is indicated by the vertical dotted line. The dashed curve in panel (b) shows the ratio between the direct photoionization cross sections (i.e., without the Fano interference).

conventional resonant Auger electrons exhibits resonance structures. This recorded resonance-enhanced yield is in agreement with the experimental results of Ref. [6] (see Fig. 1 of there). This signal was used to calibrate the exciting-photon energy.

In each individual spectrum the two nitrogen 1s-peaks were fitted by Gaussian functions. The areas of these functions yield the individual spectral intensities shown in Fig. 3a. Dividing these intensities results in the energy-dependent ratio of $N_c(1s)$ to $N_t(1s)$ shown in Fig. 3b. A residual background of the ratio can be explained by the logarithmic transmission function of the magnetic-bottle spectrometer used for this experiment. The best fit of the systematic background by a logarithmic function is also shown in Fig. 3b by the dashed curve. The measured ratio of two photoelectron intensities exhibits a Fano-interference behavior around the background curve across the O $1s \rightarrow \pi^*$ resonance at 534.6 eV [6] (see discussion in Sec. IV).

III. THEORY

In order to assign the presently observed variation in the ratio between the two photoionization yields to the Fano interference, we modeled the interatomic resonant Auger decay in N_2O theoretically. For this purpose, we applied the previously developed theoretical approach, which was successfully used to interpret core ionization and core excitation spectra of polyatomic molecules [16–22]. It includes the electronic state interference (ESI, [23]) and the lifetime vibrational interference (LVI, [24]) via the Kramers-Heisenberg formula. In the one-particle Hartree-Fock approximation, the electronic part of the total amplitude for the 1s-photoionization of nitrogen atoms in the vicinity of the O $1s \rightarrow \pi^*$ excitation reads [16, 19, 22, 23]:

$$D_{\ell mk}(\omega) = \langle \varepsilon \ell m | \mathbf{d}_k | 1s_{\rm N} \rangle + \frac{\langle 1s_{\rm O}\, \varepsilon \ell m | \mathbf{H}^{\rm ee} | 1s_{\rm N}\, \pi^* \rangle \langle \pi^* | \mathbf{d}_k | 1s_{\rm O} \rangle}{\omega - E_{\pi^*} + i\Gamma_{\pi^*}/2}. \quad (1)$$

Here, $\mathbf{H}^{\rm ee}$ is the operator for the electrostatic Coulomb interaction and $\mathbf{d}_k$ is the electric dipole transition operator for the absorption of a photon with polarization k. The one-particle wave functions of the bound states $|1s_{\rm O}\rangle$, $|1s_{\rm N}\rangle$ and $|\pi^*\rangle$ represent the respective core electrons of the oxygen and nitrogen atoms, as well as the considered excited state with the energy E_{π^*} and Auger decay width Γ_{π^*}. The photoelectron partial continuum waves with angular momentum quantum numbers ℓ and m are designated as $|\varepsilon \ell m\rangle$. The photon energy ω is related to the photoelectron kinetic energy ε and the binding energy IP of the N 1s-electron as: $\omega = IP + \varepsilon$. The total photoionization cross section is given by the incoherent sum over the partial cross sections as:

$$\sigma(\omega) = \sum_{\ell mk} |D_{\ell mk}(\omega)|^2. \quad (2)$$

The electronic transition amplitudes for the ionization, excitation and Auger decay from Eq. (1) were computed by the stationary single Center (SC) method [25, 26]. Calculations were performed in the frozen-core Hartree-Fock approximation at the equilibrium linear geometry of the neutral N_2O molecule. Wavefunction of the lowermost excited electronic state (i.e., of the LUMO) was obtained in the equivalent core "Z + 1" approximation, while contributions from highly-excited states

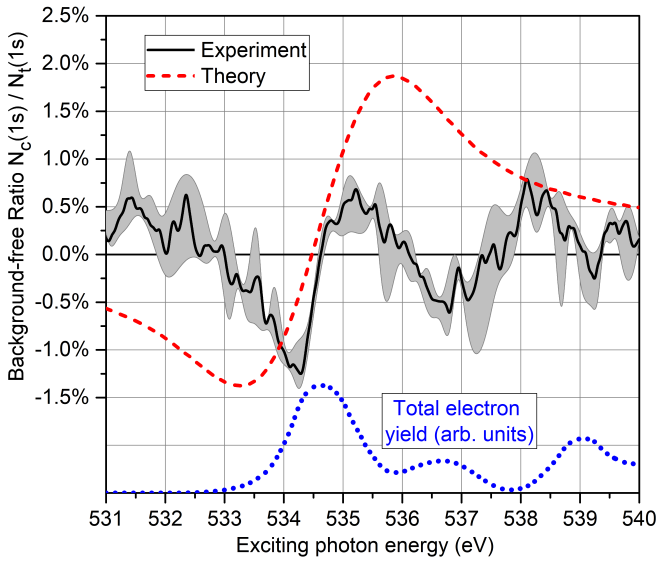

FIG. 5: Solid curve: experimental ratio between the $N_c(1s)$ and $N_t(1s)$ photoionization yields after subtraction of the logarithmic background of the transmission function (combination of the data from Fig. 3b). A five point moving average was used for the background-free ratio. The shaded area represents the maximal uncertainty derived from the statistical uncertainty (c.f. figure 3) and the resulting fit uncertainty of the logarithmic background. Dashed curve: the theoretical ratio of the respective cross sections after subtraction of the constant ratio of the direct photoionization cross sections (combination of the data from Fig. 4b). Both, the experimental and theoretical data exhibit a clear indication for a Fano-lineshape caused by the Fano interference. Note that only O $1s \rightarrow \pi^*$ resonance was included in the calculations, and at least three prominent resonant features are present in the experimental total electron yield spectrum [6] (indicated at the bottom of the figure by dotted curve, see also text for details).

of Rydberg-character were neglected. Details of the calculation can be found in our previous study of this molecule [16]. The SC expansions of the bound and continuum electrons were restricted by the partial waves with $\ell_c \leq 99$ and $\ell_\varepsilon \leq 49$, respectively. The photoionization cross sections were computed for the whole vibrationally unresolved bands of the $N_c(1s)$ and $N_t(1s)$ core-ionized states. This was realized by an analytical procedure from the appendix of Ref. [16], which requires only the shape of the excitation spectrum and keeps the Fano interference unaltered. Here, we utilized the experimental O $1s \rightarrow \pi^*$ excitation function from Fig. 1 of Ref. [6]. Results of the present calculations are collected in Fig. 4.

IV. RESULTS AND DISCUSSION

As one can see from Fig. 4a, the computed cross sections for the 1s-photoionization of the central (red curve) and terminal (black curve) nitrogen atoms exhibit very broad asymmetric Fano profiles at the position of the considered O $1s \rightarrow \pi^*$ excitation (indicated by the vertical dotted line). As also intuitively expected, the intensity variation caused by the interference in the $N_c(1s)$ cross section is considerably larger than in the $N_t(1s)$ one (because of the closer location of the former to the oxygen atom). This intensity variation is also present in the ratio between the two cross sections depicted in Fig. 4b by the solid curve. As one also can see, the computed ratio is larger than one: The ratio of the direct photoionization cross sections (i.e., without the Fano interference) is equal to 1.042, as indicated by the horizontal dashed line in Fig. 4b. This fact is in agreement with the present measurements. Indeed, in the exciting-photon energy range of interest, the experimental ratio of the $N_c(1s)$ and $N_t(1s)$ photoionization yields in Fig. 3b is larger than one. This present result is in contradiction with the previous measurements of Ref. [6], which reports an inverse ratio in between 1.1 and 1.2 (see Fig. 2a therein). Uncovering reasons of this disagreement is outside the scope of the present work.

Figure 5 depicts the presently measured background-free ratio between the $N_c(1s)$ and $N_t(1s)$ photoionization yields (solid curve with error-bars shown by the shaded area). This ratio exhibits a Fano-lineshape across the positions of the O 1s-resonances (note that the experimental total electron yield spectrum in Fig. 1 of Ref. [6] exhibits three prominent features: the $1s \rightarrow \pi^*$ excitation at 534.6 eV and two more resonances at about 536.7 and 539.1 eV, as illustrated in the bottom of Fig. 5 by the dotted curve). The experimental background-free ratio is compared in Fig. 5 with the respective theoretical ratio (dashed curve), from which the contribution from the direct photoionization channels was already subtracted (see data in Fig. 4b). As one can see, the computed ratio possesses a similar lineshape at the position of the O $1s \rightarrow \pi^*$ excitation. The variation of the computed ratio is however somewhat stronger (from about –1.4 % to +1.9 % in the theory, as compared to from –1.3 % to +0.7 % in the experiment). Since, in the experiment, the influence of the additional resonances at about 536.7 and 539.1 eV due to their widths on the line-shape of the calculated resonance at 534.6 eV cannot be disentangled, a quantitative agreement between the present computation and the experiment can, obviously, not be achieved. The agreement between the presently computed and measured ratios in Fig. 5 can be considered, therefore, as semi-quantitative.

As a final point, let us take a closer look on the respective Auger decay matrix element from Eq. (1). Its explicit expression reads:

$$\langle 1s_O\, \varepsilon\ell m | \mathbf{H}^{ee} | 1s_N\, \pi^* \rangle = - D(1s_O\, \varepsilon\ell m, 1s_N\, \pi^*) + 2E(1s_O\, \varepsilon\ell m, \pi^*\, 1s_N), \quad (3)$$

where D and E are the direct and exchange contributions to the Coulomb matrix elements. The direct contribution describes the charge transfer process (Fig. 1c), in which

an N 1s-electron closes the O 1s-hole and the excited electron is released in the continuum. The exchange matrix element represents the energy transfer process, in which the excited electron fills the O 1s-hole and the energy is transferred by a virtual photon to ionize the N 1s-electron (Fig. 1b). The present calculations uncover that for the central and terminal nitrogen atoms of N_2O the energy transfer is, respectively, by about four and five orders of magnitude more probable than the charge transfer. In particular, the presently computed partial interatomic resonant Auger decay widths are equal to $\Gamma_c = 27\,\mu$eV and $\Gamma_t = 0.46\,\mu$eV. These rates fit perfectly to the $1/R^6$ law [27], confirming the leading role of the dipole-dipole interactions ($R_{O-N_c} = 2.24$ a.u. and $R_{O-N_t} = 4.37$ a.u. [28]). If one neglects the contribution from the charge transfer process, i.e. the direct matrix element D, the respective partial decay widths decrease only by about 3 % and 1 %, respectively. Because of a localization of two core-electrons involved in the transition, this conclusion should be system-independent for the interatomic resonant Auger processes. One thus can suggest an analogy of the interatomic resonant Auger decay to the antenna-receiver mechanism [11], in which the oxygen atom serves as an antenna by efficiently absorbing the light, and the excess energy is then transferred to the nitrogen core-holes which play a role of receivers.

V. SUMMARY

Because interatomic resonant Auger decay in molecules is a rather subtle effect, its first observers concluded that it can be measurable *only* in the differential photoionization cross sections *via nondipole* photoemission [6]. A few years later [8], coincident measurements demonstrated that the effect is present in the *dipole* photoelectron angular emission distributions from fixed-in-space molecules. Those observations were explained in terms of the Fano interference between the dominant direct photoionization and very weak nonlocal resonant Auger decay channel. Recent progress made with respect to stability, flux, and resolution of the synchrotron radiation beam, combined with state-of-the-art time-of-flight spectroscopy with electron retardation, enabled a direct observation of this Fano interference in the total photoionization intensities, caused by the interatomic resonant Auger decay of N_2O. The interference results in an observable sign change of the ratio between the total $N_c(1s)$ and $N_t(1s)$ photoionization yields across the O K-edge resonances. The observations are unambiguously supported by the present theoretical model, which identifies energy transfer as the main mechanism of the interatomic resonant Auger effect.

Acknowledgments

We acknowledge DESY (Hamburg, Germany), a member of the Helmholtz Association HGF, for the provision of experimental facilities at PETRA III. This research was supported in part through the Maxwell computational resources operated at DESY. The theoretical work was supported by the DFG Project DE 2366/1-2. M.I. acknowledges funding by the Volkswagen foundation within a Peter Paul Ewald-Fellowship. A.A. received financial support from CUI at the University of Hamburg under grant number DFG EXC 1074. We acknowledge support of the theory-experiment collaboration from Deutsche Forschungsgemeinschaft via Sonderforschungsbereich SFB-1319 (ELCH) and Forschungsgruppe FOR-1789 (ICD).

[1] A. Kay, E. Arenholz, S. Mun, F. J. García de Abajo, C. S. Fadley, R. Denecke, Z. Hussain, M. A. Van Hove, Science **281**, 679 (1998).
[2] F.J. García de Abajo, C. S. Fadley, and M.A. van Hove, Phys. Rev. Lett. **82**, 4126 (1999).
[3] A.W. Kay, F.J. Garcia de Abajo, S.-H. Yang, E. Arenholz, B.S. Mun, N. Mannella, Z. Hussain, M.A. van Hove, and C.S. Fadley, Phys. Rev. B **63**, 679 (2001).
[4] A. Moewes, E.Z. Kurmaev, D.L. Ederer, and T.A. Callcott, Phy. Rev. B **62**, 15427 (2000).
[5] D. Nordlund, M.G. Garnier, N. Witkowski, R. Denecke, A. Nilsson, M. Nagasono, N. Mårtensson, and A. Föhlisch, Phys. Rev. B **63**, 441 (2001).
[6] R. Guillemin, O. Hemmers, D. Rolles, S.W. Yu, A. Wolska, I. Tran, A. Hudson, J. Baker and D.W. Lindle, Phys. Rev. Lett. **92**, 223002 (2004).
[7] R. Guillemin, O. Hemmers, D.W. Lindle, and S.T. Manson, Rad. Phys. Chem. **73**, 311 (2005).
[8] M. Yamazaki, J.-i. Adachi, T. Teramoto, and A. Yagishita, J. Phys. B **40**, F207 (2007).
[9] M. Yamazaki, J. Adachi, T. Teramoto, and A. Yagishita, J. Phys. B **46**, 115101 (2013).
[10] L.S. Cederbaum, J. Zobeley, and F. Tarantelli, Phys. Rev. Lett. **79**, 4778 (1997).
[11] B. Najjari, A. B. Voitkiv, and C. Müller, Phys. Rev. Lett. **105**, 153002 (2010).
[12] F. Trinter, J.B. Williams, M. Weller, M. Waitz, M. Pitzer, J. Voigtsberger, C. Schober, G. Kastirke, C. Müller, C. Goihl, P. Burzynski, F. Wiegandt, R. Wallauer, A. Kalinin, L.Ph.H. Schmidt, M.S. Schöffler, Y.-C. Chiang, K. Gokhberg, T. Jahnke, and R. Dörner, Phys. Rev. Lett. **111**, 233004 (2013).
[13] A. Hans, P. Schmidt, C. Ozga, C. Richter, H. Otto, X. Holzapfel, G. Hartmann, A. Ehresmann, U. Hergenhahn, and A. Knie, J. Phys. Chem. Lett. **10**, 1078 (2019).
[14] J. Viefhaus, F. Scholz, S. Deinert, L. Glaser, M. Ilchen, J. Seltmann, P. Walter, and F. Siewert, Nucl. Instrum. Methods Phys. Res., Sect. A **710**, 151 (2013).
[15] S. Deinert, *Aufbau eines hocheffizienten Photoelektron-Photoion-Koinzidenzexperiments* (University of Hamburg, Ph.D thesis, 2013). http://ediss.sub.uni-hamburg.de/volltexte/2013/6207/

[16] A. Knie, M. Ilchen, Ph. Schmidt, Ph. Reiß, C. Ozga, B. Kambs, A. Hans, N. Müglich, S.A. Galitskiy, L. Glaser, P. Walter, J. Viefhaus, A. Ehresmann, and Ph.V. Demekhin, Phys. Rev. A **90**, 013416 (2014).

[17] E. Antonsson, M. Patanen, C. Nicolas, S. Benkoula, J.J. Neville, V.L. Sukhorukov, J.D. Bozek, Ph.V. Demekhin, and C. Miron, Phys. Rev. A **92**, 042506 (2015).

[18] A. Knie, M. Patanen, A. Hans, I.D. Petrov, J.D. Bozek, A. Ehresmann, and Ph.V. Demekhin, Phys. Rev. Lett. **116**, 193002 (2016).

[19] S. Nandi, C. Nicolas, A. N. Artemyev, N. M. Novikovskiy, C. Miron, J.D. Bozek, and Ph.V. Demekhin, Phys. Rev. A **96**, 052501 (2017).

[20] M. Ilchen, G. Hartmann, P. Rupprecht, A.N. Artemyev, R.N. Coffee, Z. Li, H. Ohldag, H. Ogasawara, T. Osipov, D. Ray, Ph. Schmidt, T.J.A. Wolf, A. Ehresmann, S. Moeller, A. Knie, and Ph.V. Demekhin, Phys. Rev. A **95**, 053423 (2017).

[21] M. Tia, M. Pitzer, G. Kastirke, J. Gatzke, H.-K. Kim, F. Trinter, J. Rist, A. Hartung, D. Trabert, J. Siebert, K. Henrichs, J. Becht, S. Zeller, H. Gassert, F. Wiegandt, R. Wallauer, A. Kuhlins, C. Schober, T. Bauer, N. Wechselberger, P. Burzynski, J. Neff, M. Weller, D. Metz, M. Kircher, M. Waitz, J.B. Williams, L. Schmidt, A.D. Müller, A. Knie, A. Hans, L. Ben Ltaief, A. Ehresmann, R. Berger, H. Fukuzawa, K. Ueda, H. Schmidt-Böcking, R. Dörner, T. Jahnke, Ph.V. Demekhin, and M. Schöffler, J. Phys. Chem. Lett. **8**, 2780 (2017).

[22] G. Hartmann, M. Ilchen, Ph. Schmidt, C. Küstner-Wetekam, C. Ozga, F. Scholz, J. Buck, F. Trinter, J. Viefhaus, A. Ehresmann, M.S. Schöffler, A. Knie, and Ph. V. Demekhin, Phys. Rev. Lett. **123**, 043202 (2019).

[23] A. Cesar and H. Ågren, Phys. Rev. A **45**, 2833 (1992).

[24] F.K. Gel'mukhanov, L.N. Mazalov, and A. V. Kondratenko, Chem. Phys. Lett. **46**, 133 (1977).

[25] Ph.V. Demekhin, A. Ehresmann, V.L. Sukhorukov, J. Chem. Phys. **134**, 024113 (2011).

[26] S.A. Galitskiy, A.N. Artemyev, K. Jänkälä, B.M. Lagutin, Ph. V. Demekhin, J. Chem. Phys. **142**, 034306 (2015).

[27] V. Averbukh, I.B. Müller, L.S. Cederbaum, Phys. Rev. Lett. **93**, 263002 (2004).

[28] G. Herzberg, *Molecular Spectra and Molecular Structure. III. Electronic Spectra and Electronic Structure of Polyatomic Molecules* (Van Nostrand Reinhold, New York, 1966).